

1  
2  
3  
4  
5  
6  
7  
8  
9  
10  
11  
12  
13  
14  
15  
16  
17  
18

**Progressing Characteristics of Leader/return stroke Sequences of an  
Altitude-triggered Lightning Flash Containing 15 Attempted Leaders and 8  
Stroked Leaders**

**Jianguo Wang<sup>1</sup>, Fukun Wang<sup>1</sup>, Li Cai<sup>1</sup>, Rui Su<sup>1</sup>, Yadong Fan<sup>1</sup>, Mi Zhou<sup>1</sup>**

<sup>1</sup>School of Electrical Engineering and Automation, Wuhan University, Wuhan, China

Corresponding author: Li Cai ([caili@whu.edu.cn](mailto:caili@whu.edu.cn)); FukunWang ([@whu.edu.cn](mailto:@whu.edu.cn))

**Key Points:**

- An altitude-triggered lightning flash with 8 leader/return stroke sequences containing 15 attempted leaders and 8 stroked leaders was observed and analyzed.
- Attempted leaders are found to die out in three ways: disappear in somewhere of the path, switch to propagate along the channel of a branch, be caught up and merged by other leaders propagating along the same path.
- The critical point and the critical speed value between attempted leaders and stroked leaders are found to exist.

## Abstract

An altitude-triggered lightning flash with 8 leader/return stroke sequences containing 15 attempted leaders and 8 stroked leaders was observed with a high-speed camera and a mirrorless camera. The path and velocity characteristics of these leaders are investigated in detail. These leaders propagated along three different paths and had different development processes. Attempted leaders are found to die out in three ways: slow down and then disappear in somewhere of the path, give up propagating along the path and switch to propagate along the channel of a branch, be caught up and merged by other leaders propagating along the same path. Propagations of attempted leaders are not progressive, with some of them not always reaching as far as previous one did. The terminal height of attempted leaders ranges from over 1617m to 875m above the ground. A branching node is found to be the critical point determining a leader to attach the ground or not. Average 2-D speed of attempted leaders range from  $2.7 \times 10^5 \text{ m/s}$  to  $21.0 \times 10^5 \text{ m/s}$ . Some of attempted leaders even propagated in a higher speed than stroked leaders before they died out. There is no inevitable relation between the initial speed and their final fate. A critical value of propagation speed between attempted leaders and stroked leaders reported here is found to be  $4 \times 10^6 \text{ m/s}$ . Attempted leaders are found to slow down before propagating to the two branching nodes along the path.

## 1. Introduction

The attempted leader, which was defined to the dart leader that died out before reaching the ground, was first observed and named by Rhodes et al. (1994) using radio interferometry. Since then, researchers used radio interferometry or measured the change of electromagnetic field to speculate the existence of attempted leaders (e.g., Rhodes et al., 1994; Shao et al., 1995; Mardiana et al., 2002; Zhang et al., 2008; Yang et al., 2009). The light intensity of return stroke channel and dart leader were studied, using ALPS (Wang et al., 1999) and LAPOS (e.g., Zhou et al., 2014; Huang et al., 2019), while there are few literatures focusing on attempted leaders. The development and application of high-speed (HS) camera make the optical records of attempted leaders visualized. Lu et al. (2007) observed an attempted leader preceding the fourth return stroke using a HS camera whose frame rate was 5000 frames per second. Attempted leaders are hard to be recorded by the HS camera because most of them are hidden by the cloud opacity.

Dart leader is a type of lightning leader that occurs before the subsequent return stroke and propagates along the residual channel left by a preceding return stroke. Corresponding to the attempted leader, the stroked leader here is defined to the dart leader that has accomplished its propagation and initiated return stroke when it attached the ground. A leader/return stroke sequence here refers to a process from the occurrence of first attempted leader, after the initial stage or a preceding return stroke, to the end of a return stroke. If there are no attempted leaders occurring before a

return stroke, the origin of this leader/return stroke sequence is the occurrence of a stroke leader.

There are three main scenarios for the occurrence of attempted leaders, the first scenario is at the interval between return strokes in the natural lightning flashes, the second one is at the interval between return strokes in the artificially-triggered lightning flashes, and the third one is in the initial stage of artificially-triggered lightning flashes.

Rhodes et al. (1994) reported two attempted leaders occurring during the interval between return strokes in a downward negative cloud-to-ground (CG) flash. They occurred before the second stroke and the fifth stroke, respectively. Shao et al. (1995) observed four attempted leaders in a negative CG flash, and three of them occurred before the second return stroke while the remaining one occurred before the eighth return stroke.

Attempted leaders were also observed during the interval between return strokes in an upward negative CG flash (e.g., Jiang et al., 2014; Zhu et al., 2019) and the interval between a positive RS and a negative RS in a bipolar lightning flash (Campos et al., 2013). In artificially-triggered lightning flashes, attempted leaders were reported to occur in both initial stage (Yang et al., 2009) and the interval between return strokes (e.g., Qie et al., 2016).

Most of the reported attempted leaders propagated along the preexisting discharge channel. It is generally accepted that attempted leaders are similar with K events and dart leaders, which can be seen from the similarities of the fast-electric

field change waveforms (e.g., Rhodes et al., 1994; Zhang et al., 2008). One assumption generally accepted for their disappearance is that the insufficient energy is available to reionize the channel all the way to ground (Shao et al., 1995). Zhang et al. (2008) proposed that the occurrence of attempted leaders was to deposit charges to the channel and their origination might become the channel of next leader. In other words, attempted leaders can provide an extra preparation for the following leaders, making it easier for them to attach the ground and initiate a return stroke.

Propagation speed is a basic parameter for the progression of attempted leaders. Shao et al. (1995) reported that attempted leaders had an average 2-D speed of  $7\text{--}10\times 10^6$  m/s, five times higher than the speed of the counterparts reported by Mardiana et al. (2002). Campos et al. (2013) reported that attempted leaders propagated at a 2-D speed with the order of  $10^6$  m/s. An attempted leader observed by Lu et al. (2007) had a 2-D speed ranging from  $1.1\times 10^5$  to  $1.1\times 10^6$  m/s, and that reported by Wang et al. (2018) had an even lower average 2-D speed of  $7.4\times 10^4$  m/s.

Terminal height is a concerned parameter for the progression of attempted leaders. Wang et al. (2018) reported the terminal height of attempted leader to be just above the grounding point, while that reported by Jiang et al. (2014) was about 2400 m. For attempted leaders in the same flash, the terminal heights of them did not have a clear progressive relationship, with some of attempted leaders not always reaching as far as previous one did (Campos et al., 2013).

The altitude-triggered lightning was applied by Laroche et al. (1991) and then used by other researchers (e.g., Lalande et al., 1998; Rakov et al., 1998; Zhang et al.,

2003; Miki et al., 2005; Saba et al., 2005; Lu et al., 2008; Qie et al., 2009; Biagi et al., 2013). Both altitude-triggered lightning and classical triggered lightning consist of the initial stage and the leader/return stroke sequences. There is apparent visual difference existing in their initial stage between these two types of triggered lightning. Visualized optical records of the leader/return stroke sequences are also deserved to be investigated.

In this paper, 8 leader/return stroke sequences of an altitude-triggered lightning, which contains 15 attempted leaders and 8 stroked leaders, are reported and analyzed. Up to our learning, this is the first report for visualized optical observation of attempted leaders occurring in an altitude-triggered lightning flash. Mirrorless camera is adopted, making it possible to get high-image-resolution photos in the shorter exposure time.

## 2. Experiment Site and Instrumentation

The altitude-triggered lightning was triggered on 7 July 2019 at the Guangzhou Field Experiment Site for Lightning Research and Testing in Conghua, Guangdong, China. More information about the site can be found in Wang et al. (2019). Figure 1 is the 3-D aerial picture showing the locations of the observed flash, launch tower and observation station. The experiment site lies to the south of a hilly area. The distance between launch tower and observation station is 1549m.

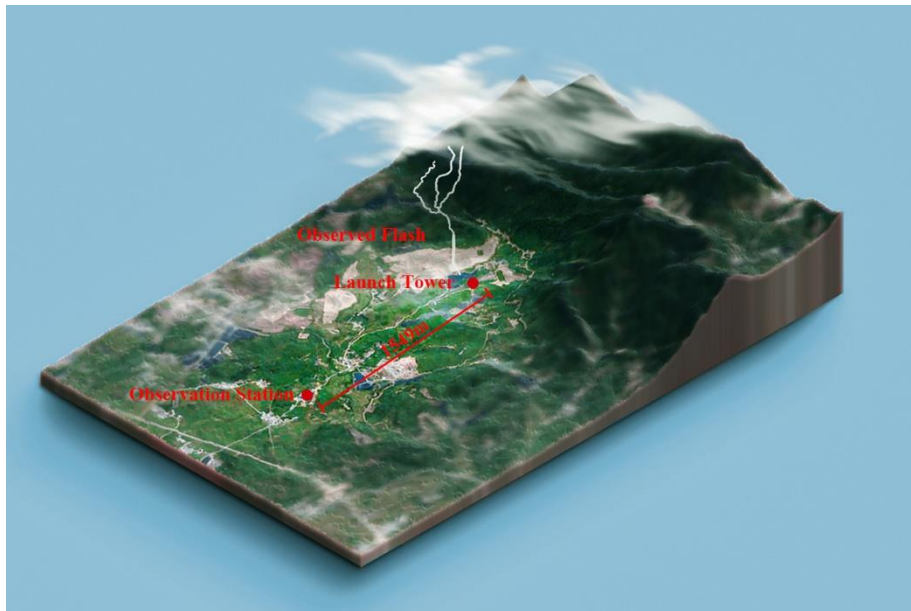


**Figure 1.** The 3-D aerial photograph showing the locations of the observed flash, launch tower and observation station. The distance between launch tower and observation station is 1549m.

The observations were performed by Engineering Research Center of Lightning Protection & Grounding Technology, Ministry of Education, China at Wuhan University. The observations were made for an attempt at classical triggered lightning that resulted in an unintentional altitude trigger after the wire broke during the ascent

period of rocket. The flash was triggered just near the launch tower according to the recorded frames, and hence the distance between it and the observation system is defined as 1549m. The height and speed discussed in following are calculated based on that.

Aiming at obtaining more comprehensive optical data, we build an integrated observation system consisting of a HS camera, a DSLR (digital single lens reflex) camera, a vidicon and a mirrorless camera. With the practical temporal resolution ranging from  $50\mu\text{s}$  to 8s, this integrated observation system can provide both high-image-resolution photos and high-time-resolution frames. Data presented here is provided by the HS camera and the mirrorless camera.

High-speed camera frames were recorded by a Phantom v2512 HS camera operating at a framing rate of 20 kfps, with an exposure time of  $49\mu\text{s}$  per frame ( $1\mu\text{s}$  dead time). The size of each pixel on the HS camera was  $20\mu\text{m}\times 20\mu\text{m}$ , and the resolution was  $640\times 608$  pixels (horizontal $\times$ vertical). The HS camera was coupled with a Nikon 16 mm lens (the f number used here was  $f / 2.8$ ) and was located on the roof of a five-story building (observation station) positioned 1549m south to the launch tower. At this distance, the spatial resolution was about 1.94m per pixel, and the field of view (FOV) was about 1242m horizontally and 1180m vertically.

High-image-resolution photos were recorded by a Lumix G9 camera. The G9 camera was operated at a framing rate of 60 fps, producing photos with a resolution of  $3888\times 5184$  pixels (horizontal $\times$ vertical). It is worth noting that the application of G9 camera helps us to obtain a high-image-resolution frame sequence instead of a single



155 high-image-resolution photo obtained by making a camera operating on the long  
156 exposure time mode. Therefore, the frames recorded by this camera have a shorter  
157 exposure time of 16.67ms without any sacrifices on image quality. This camera was  
158 located beside the HS camera and coupled with a 12-60 mm lens at f/8. The focal  
159 length used here was 12mm.

160

### 3. Data Presentation

#### 3.1 Data Overview

Figure 2 is the relative integrated luminosity of the leader/return stroke sequences in this negative altitude-triggered lightning flash. The relative luminosity is the integral of all the brightness of pixels in the HS frames, with the background brightness removed. The eight higher pulses are caused by eight return strokes, named R1 to R8, initiated by the corresponding leaders. There are 15 attempted leaders and 8 stroked leaders, named L1 to L22b, indicating that the whole process consists of 23 leaders.

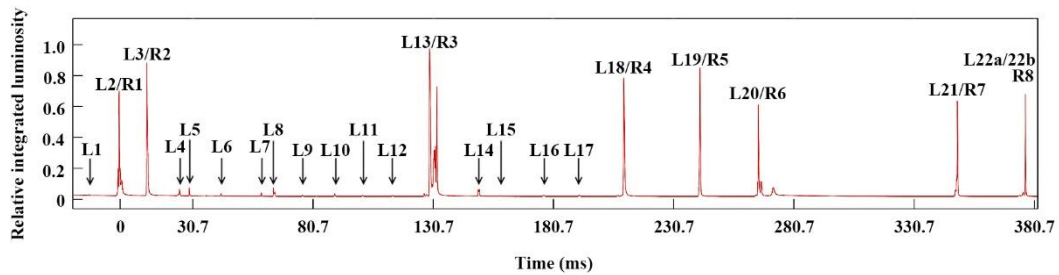


**Figure 2.** The relative integrated luminosity of the leader/return stroke sequence in this flash. The eight higher pulses are eight return strokes. L22a and L22b occurred one after another and then combined with each other.

We identify them as leaders instead of streamers due to all of them have a continuous and luminous development process, travelling a relatively long distance with the shortest one travelling more than 200 meters. These leaders are numbered in the chronological order of their occurrence.

L22a and L22b are two leaders occurring one after another in a short time and

having an interaction. Figure 3 shows development of L22a and L22b recorded by the HS camera, with frame cropped, intensity inverted and contrast enhanced. Among these 23 leaders, 8 of them are stroked leaders connecting to the ground and initiating return strokes, while 15 of them are attempted leaders which did not propagate to attach the ground. For the convenience of description, we define the time corresponding to the “first-return-stroke frame” as the time origin. In other words, the serial number of the frame where the first return stroke began is 0. There was no upward connecting leader recorded in this observation.

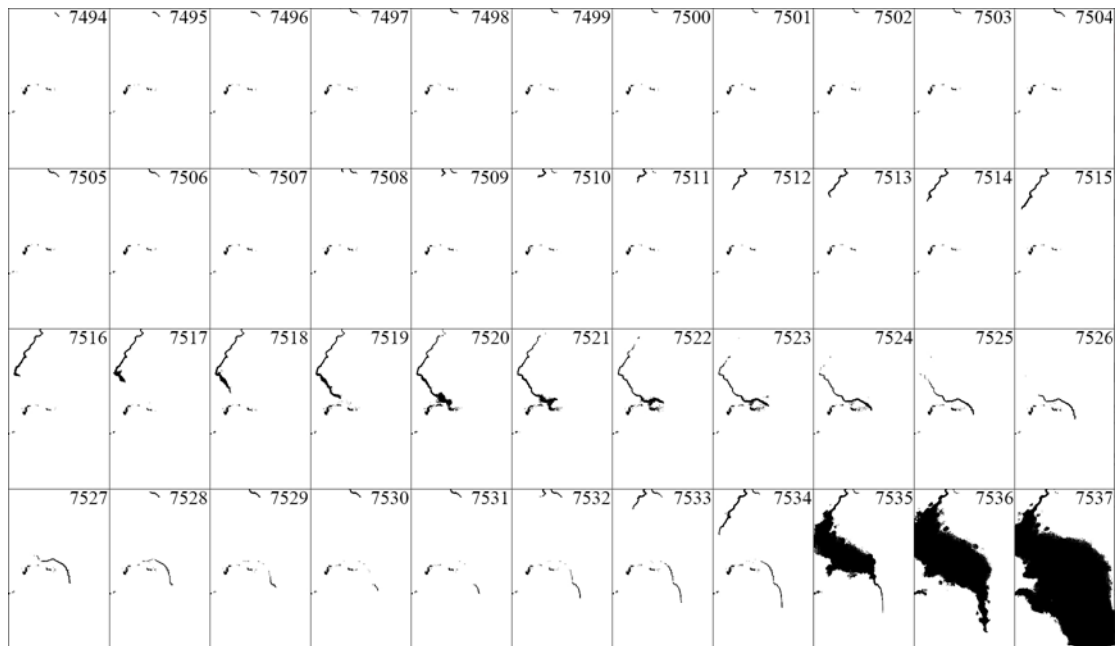


**Figure 3.** The sequence of 44 cropped frames recorded by the HS camera at 20 kfps showing the development L22a and L22b, with intensity inverted and contrast enhanced. L22a appeared first and then was caught up by L22b in frame 7535. L22a showed the bidirectional characteristic in frame 7532-7535. The composite leader connected to the ground and initiated a return stroke in frame 7537.

The path in this paper refers to the residual channel, which was created by preceding leaders in the initial stage and then traversed by leaders discussed here. In order to make the description for paths of these leaders more logical and convenient, here we give a brief review on the initial stage of this altitude-triggered lightning.

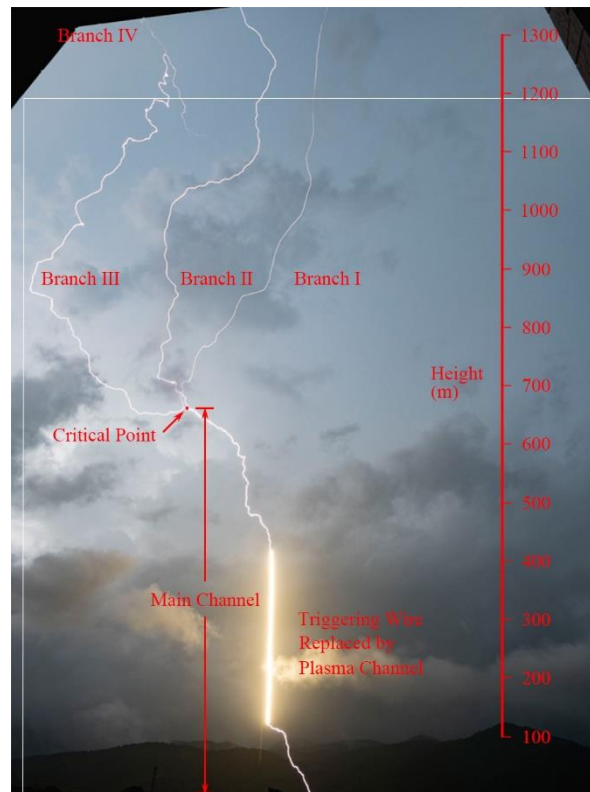


**Figure 4.** A frame recorded by G9 camera showing the initial stage of this altitude-triggered lightning. The white rectangle shows the approximate FOV of HS camera. The discharge channel is divided into a main channel and four branches.

A frame captured by G9 camera showing this initial stage is illustrated in Figure 4, with a white rectangle representing the approximate common FOV of the HS camera and the G9 camera. When the rocket ascended to a height of 400m above the ground, an upward positive leader was initiated from the top of wire that connected to the rocket. After 7.65ms, a downward negative leader occurred near the bottom of

209 released wire and then propagated toward the ground with branches. When the  
210 downward negative leader attached the ground without any upward connecting  
211 leaders observed, the so-called mini-return stroke (Zhang et al., 2003) occurred with a  
212 light wave propagating upward along the channel rapidly according to HS camera  
213 frames. The light wave traversed, illuminated the wire, and then caught up the upward  
214 positive leader that had been developing continuously since its occurrence. The  
215 injection of this light wave gave rise to 7 branches along the channel of upward leader,  
216 with most of them died out soon. Together with the upward leader itself, two of these  
217 branches survived and formed the three upper branches (named Branch I, Branch II  
218 and Branch III) for the discharge channel. The continuing current phase began shortly  
219 after these three branches extended out of the FOV of G9 camera.

220 It can be found in Figure 4 that Branch III continued its propagation for a  
221 relatively long time after leaving the FOV of HS camera and produced a new branch  
222 named Branch IV developing upward with a lower luminosity. After creating the new  
223 Branch IV, Branch III turned to propagate downward, entering the FOV of HS camera  
224 again and then shifting its direction to spread towards the right. This initial stage  
225 lasted for about 340ms till the occurrence of leader L1.

226 The analysis in following is based on the frames recorded by the HS camera. The  
227 23 leaders discussed here propagated along three different paths, named Path  $\alpha$ , Path  $\beta$   
228 and Path  $\gamma$ . We draw the three paths in different colors and separate them artificially in  
229 a composite frame as shown in Figure 5a. The composite frame is a superposition of  
230 selected frames recorded by the HS camera for the development of the 23 leaders.

Some key points along these paths are marked out in Figure 5b. It can be learned from Figure 5 that Path  $\alpha$  starts at point A and ends at point K, Path  $\beta$  starts at point B and ends at point K, Path  $\gamma$  starts at point C and ends at point K. Path  $\alpha$  and Path  $\gamma$  are two derivatives of the channel “Branch III-Main Channel” in Figure 4, while Path  $\beta$  is same with the channel “Branch I-Main Channel”.

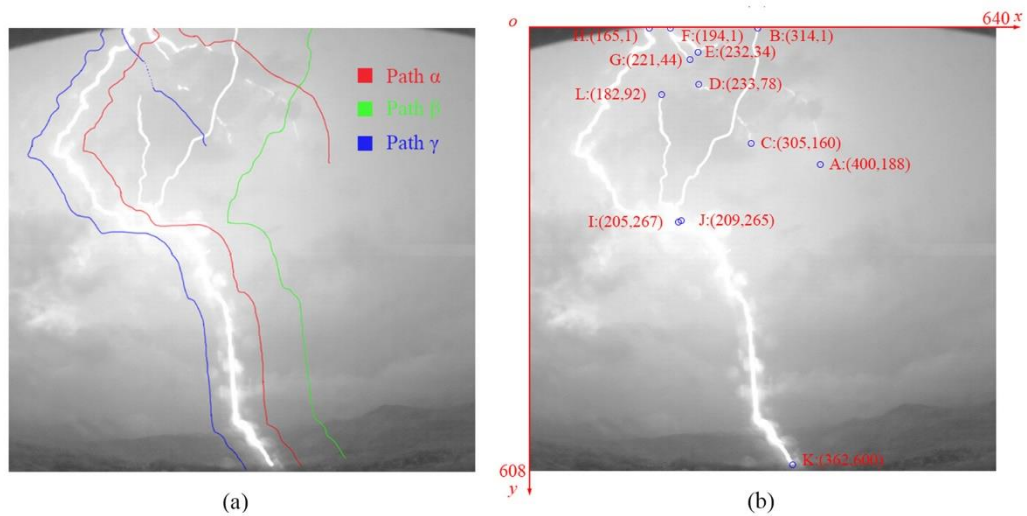


**Figure 5.** Two composite images showing the three paths of these 23 leaders, with some key points marked. (a) The three paths separated in different colors. (b) The origin in the upper left corner of the image. Point F, point I and point J are branching nodes.

The 23 leaders are categorized into three groups based on their development paths. Group Path  $\alpha$  consists of L2 and L5. L2 is a stroked leader, while L5 is an attempted leader. Group Path  $\beta$  consists of L3 and L7. L3 is a stroked leader, while L7 is an attempted leader. Group Path  $\gamma$  consists of L1, L4, L6, L8 to L21, L22a and L22b. L13, L18 to L21 and L22b are stroked leaders, while the remaining leaders are attempted leaders.

248

249

Table 1. A Summary for Main Characteristics of the 23 Leaders

Table 1. The characteristics of leader processes										
Number	Group	Occurrence Time ( ms )	Duration ( ms )	Speed ( $\times 10^3$ m/s )			Initiate return stroke or not	Degree of completion <sup>a</sup>	Terminal height ( m )	Leader interval(ms)
				Maximum	Minimum	Average				
1	C	-12.75	1.05	7.14	1.40	3.68	X	20.00%	1072	N/A
2	A	-1.15	1.20	68.97	5.72	20.75	O	100%	0	11.60
3	B	11.30	0.25	92.74	20.17	49.69	O	100%	0	12.45
4	C	24.00	1.55	24.49	4.17	10.10	X	63.00%	854	12.70
5	A	28.90	1.35	19.85	0.87	6.63	X	27.00%	> 1180	4.90
6	C	42.00	0.95	4.73	0.55	2.72	X	21.00%	1152	13.10
7	B	59.15	0.25	37.68	2.48	21.02	X	41.00%	689	17.15
8	C	64.00	1.20	21.07	1.16	10.65	X	61.00%	625	4.85
9	C	76.00	0.50	8.78	1.40	5.05	X	22.00%	> 1180	12.00
10	C	89.40	0.40	10.71	3.12	6.73	X	22.00%	> 1180	13.40
11	C	101.10	0.55	8.53	1.98	4.44	X	22.00%	> 1180	11.70
12	C	113.55	0.70	8.29	1.40	4.04	X	22.00%	> 1180	12.45
13	C	126.70	2.35	54.39	3.03	10.35	O	100%	0	13.15
14	C	149.20	1.00	26.80	3.19	10.48	X	63.00%	685	22.50
15	C	158.40	0.40	N/A	N/A	N/A	X	13.00%	999	9.20
16	C	176.15	1.40	10.17	1.40	3.90	X	32.00%	1005	17.75
17	C	191.05	1.60	11.17	0.55	3.45	X	31.00%	1034	14.90
18	C	207.15	2.70	41.07	2.79	9.03	O	100%	0	16.10
19	C	240.85	0.70	85.59	5.50	32.95	O	100%	0	33.70
20	C	264.60	1.30	42.27	3.29	19.31	O	100%	0	23.75
21	C	347.45	1.20	43.51	3.03	18.65	O	100%	0	82.85
22a	C	374.20	2.60	27.72	2.74	8.39	X <sup>b</sup>	N/A	N/A	26.75
22b	C	376.15	0.75	103.09	4.04	37.62	O <sup>b</sup>	100%	0	1.95
<sup>a</sup> The degree of completion is calculated by dividing the length of a leader by the length of the path ( the portion out of the FOV of HFS camera is not included in the calculation )										
<sup>b</sup> We treat Leader 22a as an attempted leader and accredit Leader 22b with the inducement of the return stroke										

250

251

Characteristics of the 23 leaders are summarized in Table 1. Parameters in Table

252

1 were determined as follow. The occurrence time is the time of the first occurrence of

253

each leader, relative to the time origin defined before. The leader duration is the

duration of each leader, and the duration of an attempted leader is from the first to the last occurrence of it, while that of a stroked leader is from the first occurrence of it to the beginning of the initiated return stroke. The degree of completion is a parameter calculated in the way of dividing the length of each leader by the length of the corresponding path, and the portion out of the FOV of HS camera is not included in the calculation. The terminal height is the height above the ground corresponding to the last head tip of leader before it disappeared or connected with the ground. The leader interval is the time interval between two successive leaders calculated based on the occurrence time of each leader.

### 3.2 Progressing Characteristics of leaders in Group Path $\alpha$ & Path $\beta$

We draw the three paths with some blue dotted broken lines in Figure 6, and red broken lines and arrows reflect the overall process of each leader in this group. The branches (if any) are reflected by some green broken lines and arrows. Figure 6 can tell us where these leaders branched, and how far they propagated if they were attempted leaders. To investigate the difference between stroked leaders and attempted leaders, we divide the three paths into 10 parts (see Figure 7) and calculate the average 2-D speed of leaders when they traversed these 10 path components, as shown in Figure 8.

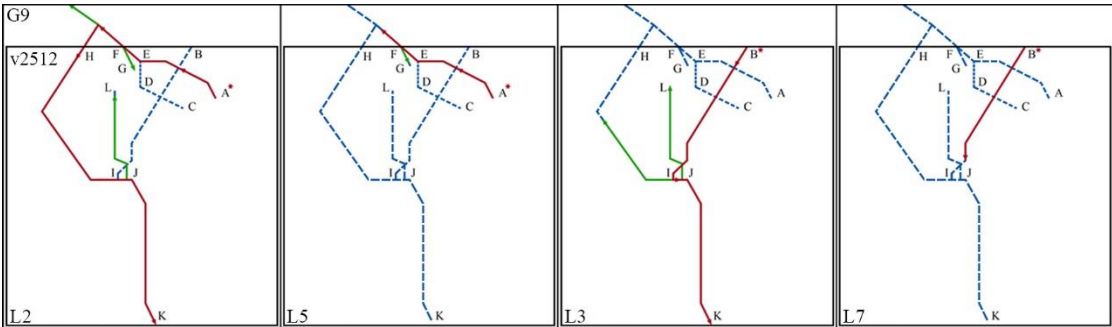




**Figure 6.** The image showing the overall process of each leader in Group Path  $\alpha$  & Path  $\beta$ . The paths, development process and branches are reflected by the blue, red and green lines. The development process out of the FOV of HS camera (V2512) is a conjecture.

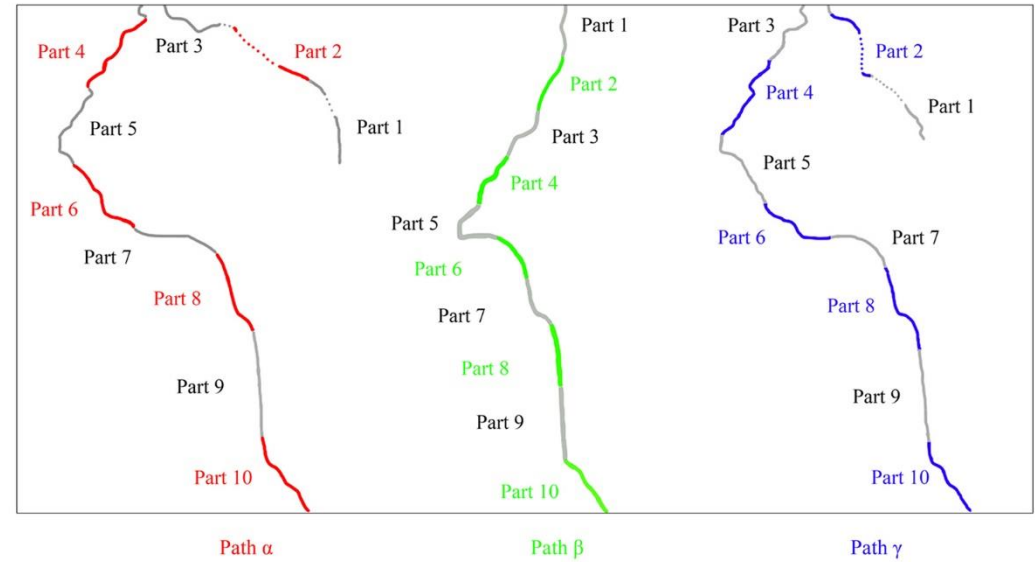


**Figure 7.** An image showing the ten parts of each path (the portion out of the FOV of HS camera is not included).

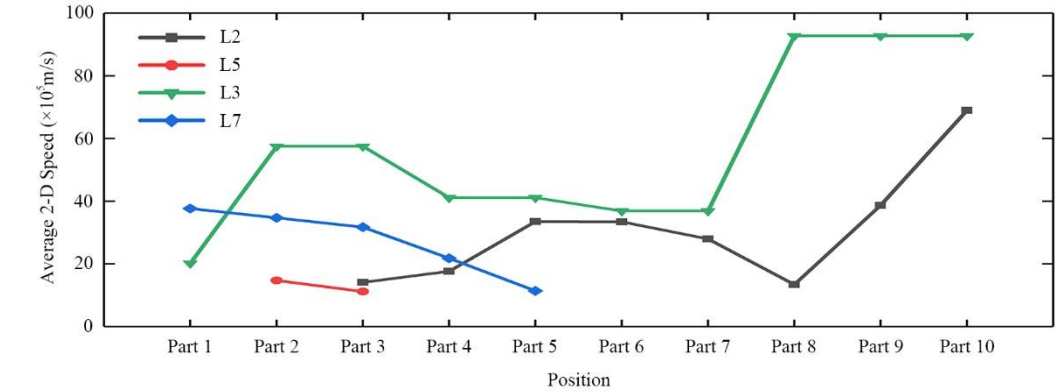


**Figure 8.** The average 2-D speed variation of leaders in Group Path  $\alpha$  & Path  $\beta$ .

The two leader processes in Group Path  $\alpha$  & Path  $\beta$  share a common

characteristic that the former one propagated with a relatively higher speed to attach the ground, while the latter one did not make it and turned to be an attempted leader.

In Group Path  $\alpha$ , both L2 and L5 produced a branch extending transiently towards point G when they propagated to point F, a branching node. The branching node here refers to a node in the path where a branch is produced. L5 died out somewhere not long after it left the FOV of HS camera, while L2 continued its propagation and probably produced a branch extending along Branch IV. There was another branch occurring transiently when L2 propagated to point J, a branching node. All branches, discussed during the leader/return stroke sequences, extended along the residual channel instead of virgin air.

Interestingly, the recorded leader channel in frames became overexposed when L2 propagated between point H and point I. The phenomenon of channel getting to be overexposed usually happens during the ground-attachment process and return stroke/continuing current stage. The channel of L2 becoming overexposed so “early” seems to mean that there exists an intense discharge process before L2 made a connection with the ground.

In Group Path  $\beta$ , L3 produced two branches while L7 died out before reaching any branching nodes. L3 was an intense leader propagating along a relatively smooth path at an average 2-D speed of  $4.97 \times 10^6$  m/s, producing the transient branches at every branching node and getting overexposed before attaching the ground.

The velocity characteristic of leaders in Group Path  $\alpha$  & Path  $\beta$  is shown in Figure 8. There may be errors in the first and last data of few curves. These errors

result from the fact that we cannot know the exact duration corresponding to leaders' first and last occurrence in the frame.

In Group Path  $\beta$ , with the exception of the first and last data, L3 and L7 share a similar varying tendency in the same positions, while L3 has a higher speed. In Group Path  $\alpha$ , due to the short life of L5, there are few conclusions reflected, but we can see that L2 and L5 share a similar speed in Part 3.

Taking these two stroked leaders into consideration, it can be found that L3 has a higher speed than L2. It may be caused by the smaller tortuosity of Path  $\beta$ . At the same time, although they have an opposite varying tendency in the middle stage, they both experience a significantly sharp increase in velocity when they are going to attach the ground. For these two attempted leaders in Figure 8, it can be found that both of them propagated with a speed lower than  $4 \times 10^6$  m/s.

### **3.3 Progressing Characteristics of leaders in Group Path $\gamma$**

Figure 9 illustrates the overall processes of leaders, and Figure 10 shows the velocity variations of them in Group Path  $\gamma$ . The leaders in Group Path  $\gamma$  are two sets of leader/return stoke sequences with some attempted leaders ahead of them for a preparation.

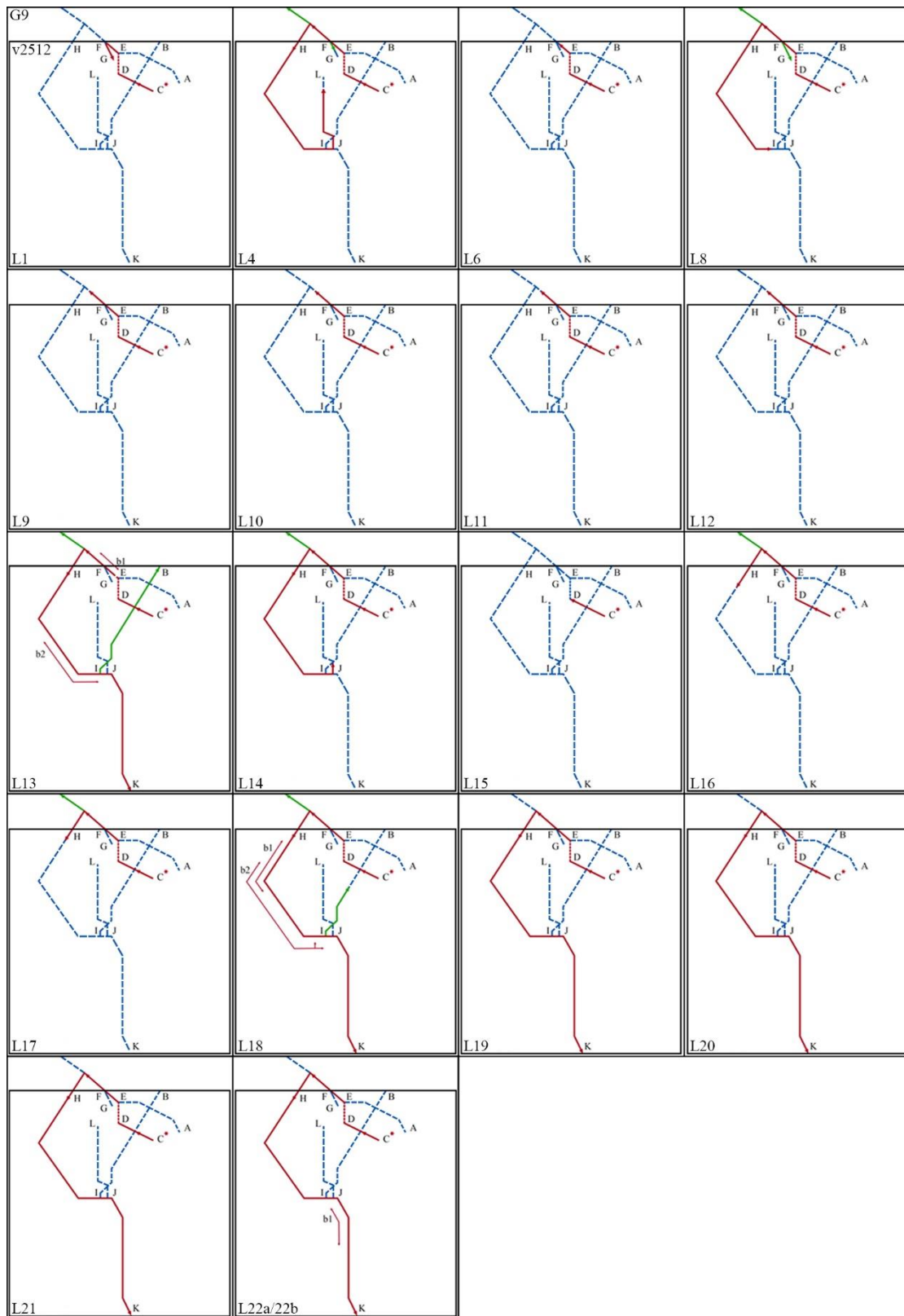


**Figure 9.** The image showing the overall process of each leader in Group Path  $\gamma$ . The paths, development process and branches are reflected by the blue, red and green lines.

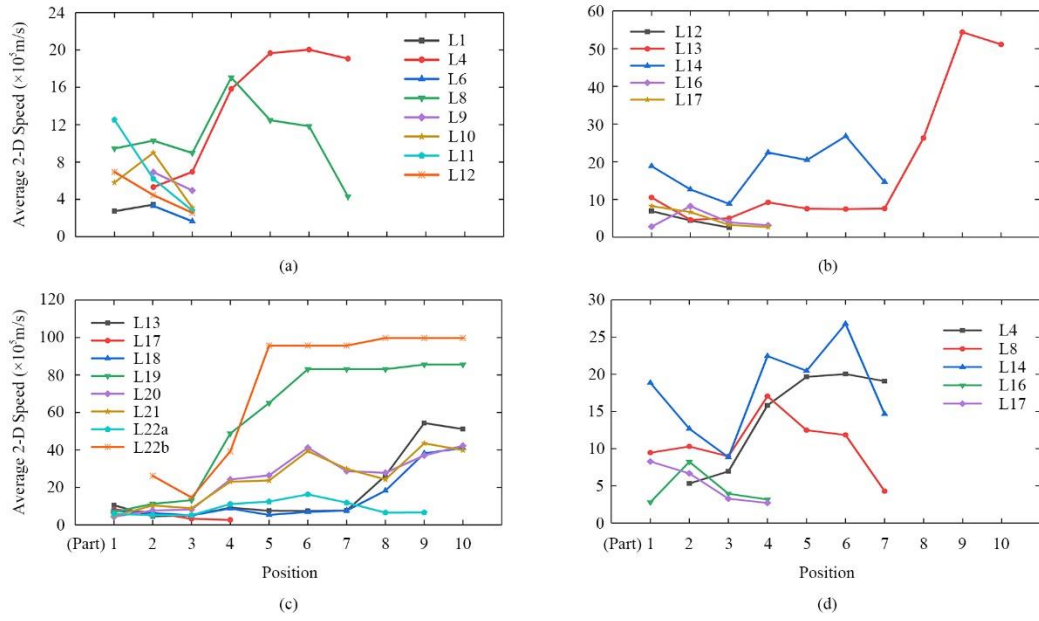


**Figure 10.** The average 2-D speed variation of leaders in Group Path  $\gamma$ . (a) The 8 attempted leaders before the first stroked leader. (b) The first stroked leader, three attempted leaders behind it and their counterpart. (c) The last 6 leaders and their counterparts. (d) The five attempted leaders surviving to enter the FOV of HS camera again.

In this group, L1, L4 and L8 produced a branch extending transiently towards point G when they propagated to point F, a branching node, while L9 to L22b traversed point F without any visible branches. Taking those leaders in Group Path  $\alpha$  & Path  $\beta$  into consideration, we can find that every leader had produced such a transient branch if they could propagate near point F, till the occurrence of L9. As mentioned above, point J is a branching node and there is another branching node, point I, near it. Equally, we can find that every leader, including leaders in Group Path  $\alpha$  & Path  $\beta$ , had produced a transient branch extending upward if they could propagate

to point I or J, till the occurrence of L19. L19 to L22b developed without any branches observed. There may be some branches produced out of the FOV of HS camera (e.g., branches developing along Branch IV).

For these attempted leaders, we can divide them into three types based on their terminal points. Firstly, L1, L6 and L15 apparently died out before point F. Secondly, L9 to L12 slowed down and disappeared out of the FOV of HS camera. Finally, L4, L8, L14, L16 and L17 entered the FOV of HS camera again but could not develop continuously to make a connection with the ground. Meanwhile, there seems to exist an impassable node, point J, in the path for these attempted leaders. All attempted leaders failed to continue the propagation along the path before or at point J.

There are also some interesting phenomena during their propagations. The channel of L13, L18 to L21 and L22b got overexposed before attaching the ground, just as L2 and L3 had done before. That is to say, all stroked leaders here have a more intense propagation process than normal dart leaders. Especially, the overexposed phenomenon of L13 once covered the branching behavior occurring at point I. The branch produced here survived to be a component of the discharge channel for the following return stroke and continuing current. At the same time, some of these stroked leaders showed the bidirectional characteristic during their development. We mark out the approximate position where the bidirectional characteristic first appeared in Figure 9. It can be found that the bidirectional characteristic appeared for twice during the development of L13 and L18, because the former one sustained for only few of frames while the latter one continued till the establishment of channel for

return stroke. L22a shows the bidirectional characteristic only once for a different reason. L22a is a special attempted leader that died out in a way of being chased and merged by another leader, L22b, propagating along the same path. The development of them recorded by the HS camera is illustrated in Figure 3 with cropped, intensity inverted and contrast enhanced. First came the L22a at 374.20ms with a relatively weaker propagation process. It is clear that L22a is a leader instead of a streamer because it has a continuous propagation process and a long luminous channel. Then came the L22b propagating along the same path but with a significantly higher speed. When the L22a was nearly overtaken by L22b, it showed the bidirectional characteristic to welcome the arrival of L22b. The overexposed phenomenon occurred when they met each other and the composite leader propagated in the bidirectional way transiently. Before the composite leader connected to the ground, it turned to propagate in a unidirectional way and then initiated a return stroke.

Figure 10 shows the average 2-D speed of leaders of this group in different parts of the path. Figure 10a illustrates the results of first 8 attempted leaders preceding the first stroked leader in Group Path  $\gamma$ . All these leaders developed with a speed lower than  $3 \times 10^6$  m/s. Leaders that died out before entering the FOV of HS camera again share a decreasing tendency, except for L1 and L10. L4 and L8 survived to enter the FOV of HS camera again, but they behaved differently on velocity property. The speed of L4 increases continuously most of the time and turns to decrease in Part 7, where L4 gave up propagating along Path  $\gamma$  and changed to develop along the channel “J-I”. By contrast, the speed of L8 fluctuates and has an earlier decrease. Figure 10b

386 illustrates the results of the first stroked leader and three attempted leaders behind it.  
387 L12 is shown again for comparison and L15 is absent because of its quite weak  
388 development process. Firstly, we can see that these three attempted leaders still  
389 propagated with a speed lower than  $3 \times 10^6 \text{m/s}$ . Secondly, compared with these  
390 attempted leaders, L13 does not show any obvious advantages in initial velocity or  
391 accelerating trend. Thirdly, it is strange that L13 shows a decrease in average 2-D  
392 velocity just before making a connection with the ground. It should be noted that this  
393 abnormal decrease is not caused by the unknown exact duration corresponding to the  
394 last length, because here we abandon this value and choose the penultimate value.  
395 Finally, considering the error existing in the first data, L16 and L17 may share a  
396 similar varying tendency among the same positions. Figure 10c illustrates the results  
397 of the remaining 6 leaders, with 5 of them are stroked leaders. L13 and L17 are shown  
398 again for a comparison. Firstly, the 5 stroked leaders behave quite differently on  
399 velocity property and seem to have no obvious relation with the chronological order.  
400 Secondly, these leaders have a similar initial velocity of about  $1 \times 10^6 \text{m/s}$ . Thirdly,  
401 L20 and L21 share a similar variation curve with some fluctuations. Fourthly, the  
402 speed of L19 and L22b increase sharply in the middle stage and then keep it to the  
403 end. Fifthly, with the preparation made by L22a, L22b has an apparently higher speed  
404 and sharper accelerating tendency. Finally, we can see that L21 shows the same  
405 decrease just before attaching the ground as L13 does. This decrease is also not  
406 caused by the error mentioned before. Figure 10d reveals the results of five attempted  
407 leaders surviving to enter the FOV of HS camera again. Although these attempted



408 leaders have some similarities in propagation processes, they do not share too much in  
409 common in terms of velocity. As mentioned before, L16 and L17 are similar leader  
410 processes and have the speed varied in consistent. However, L4 and L14 which  
411 propagated similarly do not have such a consistency. It is probably caused by the  
412 longer time interval and the occurrence of the return stroke initiated by L13.  
413

## **4. Discussion**

### **4.1 Three Termination Ways of Attempted Leaders**

After a review of all these 15 attempted leaders, we can conclude that they died out in three ways as shown in Figure 11. The first and the most common way is that they slow down gradually with decreased luminosity and then disappear in somewhere of the path as shown in Figure 11a. L5-12 and L15-17 are leaders dying out in this way. The second way is that they give up propagating along the path when they develop to a branching node and turn to extend in the channel which should have been a branch, as shown in Figure 11b. In other words, different from other leaders which produce a branch and keep propagating along the path at the same time, these leaders make a choice between the branch and the path. L1, L4 and L14 made such a choice and hence died out. The last and the rarest way is that they are caught up and merged by other leaders propagating along the same path before reaching the ground, as shown in Figure 11c. Only L22a is found to die out in this way here.

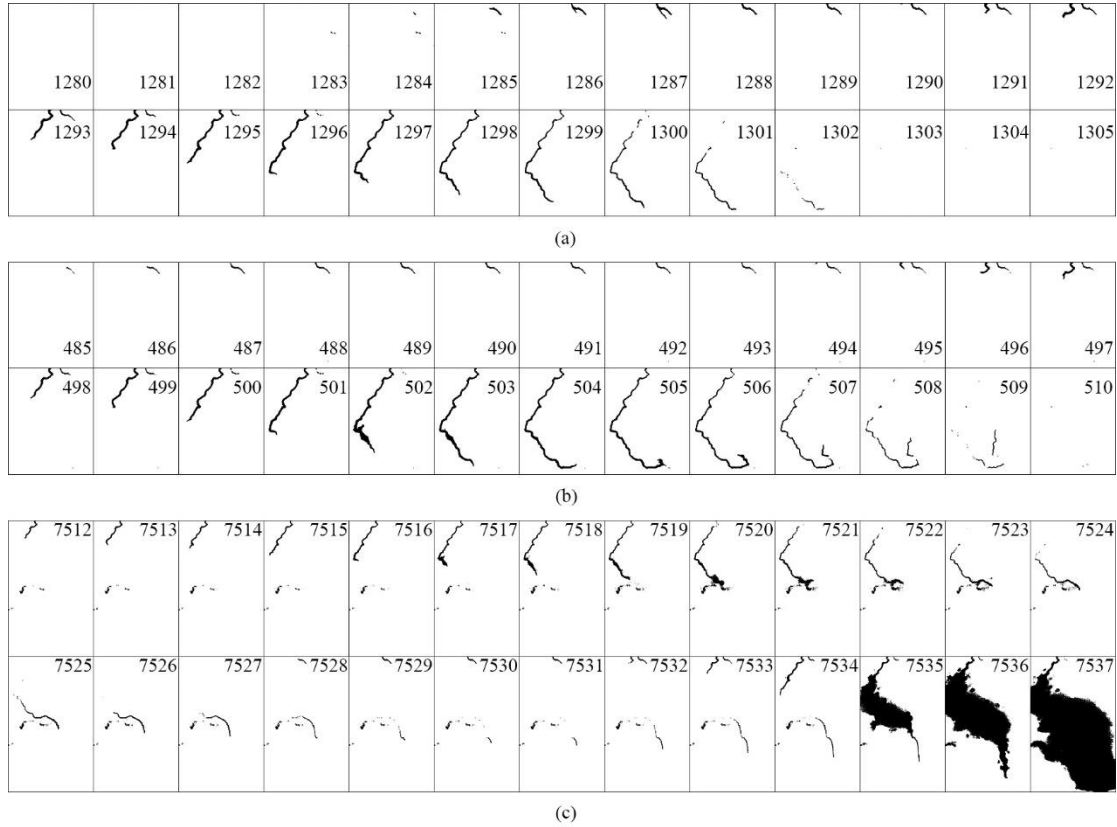


**Figure 11.** The sequence of cropped frames recorded by the HS camera showing the three termination ways, with intensity inverted and contrast enhanced. (a) The sequence of 26 frames selected from the development of L8 showing the first termination way. (b) The sequence of 26 frames selected from the development of L4 showing the second termination way. (c) The sequence of 26 frames selected from the development of L22a and 22b showing the third termination way.

## 4.2 The Critical Speed Value between Stroked Leaders and Attempted Leaders

The first termination way can be ascribed to the insufficient energy input of these leaders (Shao et al.,1995; Zhang et al.,2008). After a review of Figure 8 and Figure 10, we can find that not every attempted leader dying out in this way has a continuously downward trend in average velocity. Some of them, like L10 and L16, once

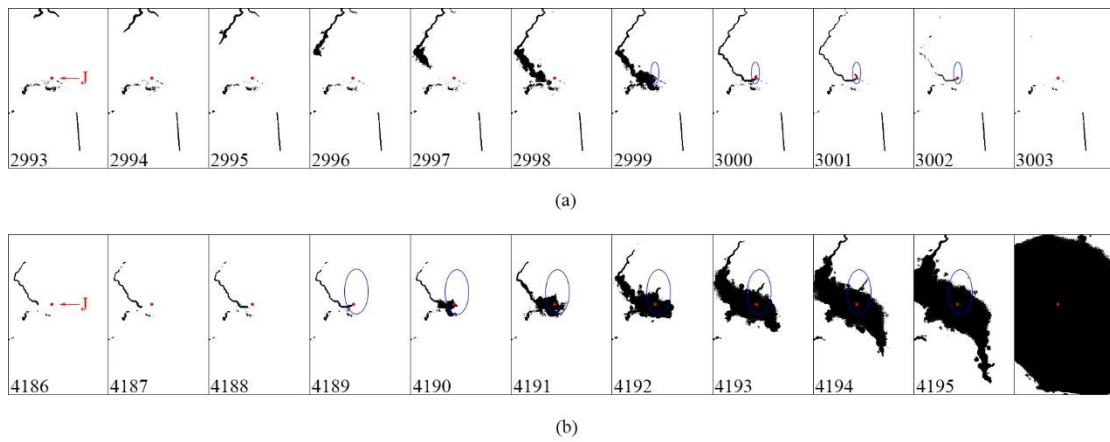
accelerated between Part 1 and Part 2 where existed clouds, indicating they may experience another process of energy input there. What's more, the initial velocity of leaders seems to have no inevitable relationship with the final fate of them. For example, L7 has a higher initial velocity than L3, and L14 occurred with a higher speed than L13, while this early advantage is not enough to make them successful. The two leaders, which have a higher initial velocity but die out finally, share a similarity that they are the first leader following a return stroke in their own path. This indicates that the higher initial velocity of them may be caused by the better development conditions of their channel with a higher temperature, lower density and better conductivity left by a preceding return stroke.

The fluctuating velocity trend and the non-inevitable relationship between initial velocity and development prospect seem to indicate that there may exist other factors influencing the disappearance of attempted leaders. By comparing Figure 8 and Figure 10, we can conclude that the real watershed between the stroked leaders and attempted leaders is the average speed value of  $4 \times 10^6 \text{ m/s}$ . All these attempted leaders, no matter how much time they had accelerated, still propagated with an average speed of less than  $4 \times 10^6 \text{ m/s}$ . For the stroked leaders, once they reached this speed value, they were bound to attach the ground even they slowed down before it.

### **4.3 The Critical Point between Stroked Leaders and Attempted Leaders**

The second termination way is related to the branching node and point J is a critical point between stroked leaders and attempted leaders. In Figure 12, we make a comparison for the behavior of one stroked leader and one attempted leader when

463 they developed to point J. It is clear that a leader will attach the ground if it can  
 464 traverse the point J and keep propagating downwards. This conclusion can be  
 465 confirmed by the development of all stroked leaders. Back to Figure 4, it can be found  
 466 that the point J is the original branching node, in the initial stage, where the upward  
 467 positive leader began to branch. Point J is located about 300m to the upper left of the  
 468 plasma channel left by the exploded wire.



469

470 **Figure 12.** Two sequences of 11 cropped frames recorded by the HS camera,  
 471 showing the different behaviors of leaders when they propagated to a branching node.  
 472 The black line in the lower middle of frame 2993-3003 is caused by the residual  
 473 luminosity of the plasma channel. (a) L14 giving up propagating along the path and  
 474 turned to extend along the channel which should have been a branch. (b) L13  
 475 propagating along the path and made a branch at the same time. The branch was not  
 476 produced at point J but L13 traversed point J later.

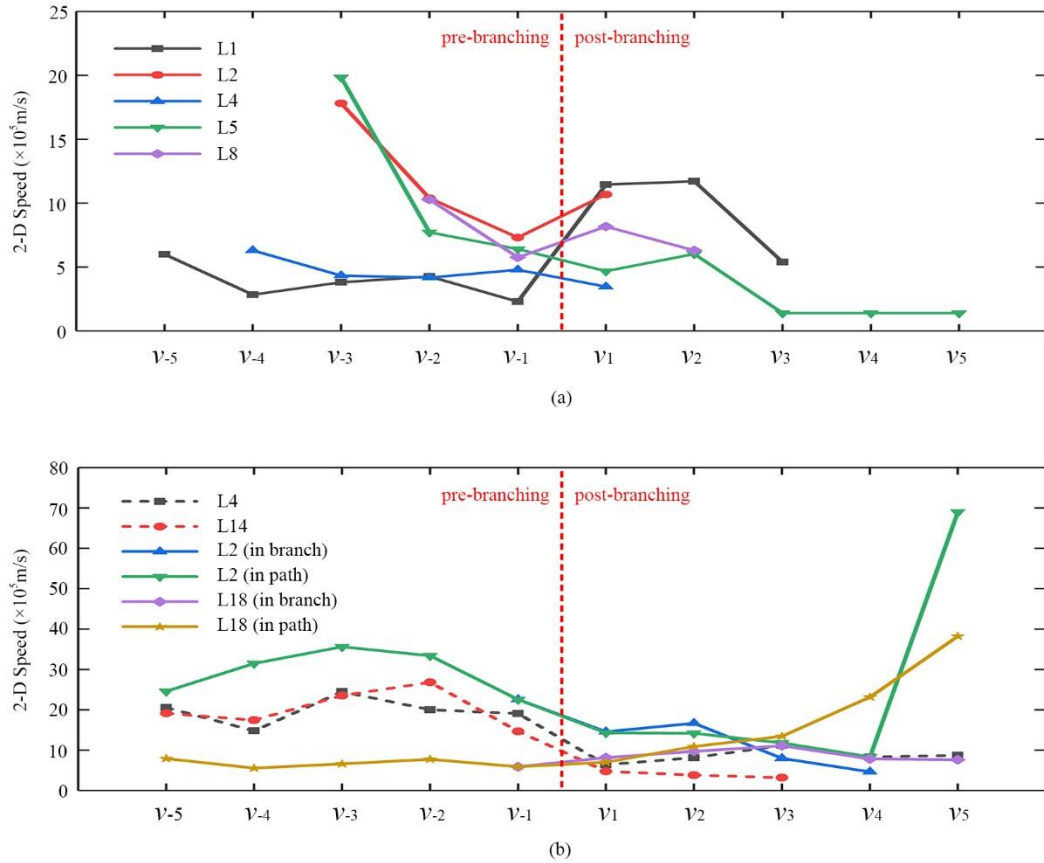


**Figure 13.** The 2-D speed variation of leaders propagating near two branching nodes. The speed is calculated between two consecutive frames. The red dotted line indicates that a branch is produced here. (a) The 2-D speed variation of leaders propagating near point F. (b) The 2-D speed variation of leaders propagating near point I and J.

For a better investigation of the branching behavior, we calculate five speed values of leaders before and after the branch producing and show the results in Figure 13. Figure 13a illustrates the branching behavior occurring near the point F while Figure 13b illustrates that occurring near the point I and point J. Only the speed of branches is calculated in the right half part in Figure 13a, because point F is on the border of FOV of HS camera. Figure 13a reveals that most of the leaders slowed

down before producing a branch, except L4. What's more, some of them once accelerated in the channel of a branch, indicating that these leaders did not branch with no reason. The situation in Figure 13b is much more complicated but we can still find the same conclusion that these leaders slowed down before the branching node. Branches or the leader itself of L2, L4 and L18 also show an acceleration lasting longer or shorter, while L14 made a totally wrong choice at point J to die out in channel "J-I" rapidly without any acceleration processes. At the same time, we can find that the branch produced by L2 decelerated together with L2 itself, while the branch produced by L18 once accelerated together with L18 itself and then turned to decelerate. It can also be seen from Figure 13b that these branches were not prevented directly by the attaching process between leaders and the ground but had already slowed down before this process.

#### **4.4 How Does a Return Stroke Influence the Following Leader Processes**

The influence, exerted by a return stroke, on the following leaders may be complex. As discussed above, a preceding return stroke can bring a better development condition for the following leaders. For example, both L4 and L14 occurred next to a return stroke occurring along the same path, and then they made a giant step forward compared with the corresponding leaders before the return stroke. However, the existence of a return stroke may also be the key factor hindering these leaders' further development. It can be learned from Figure 2 that L13 has a longer and more intense return stroke/continuing current phase, indicating that more charge was transferred to the ground. The successive occurrence of return strokes, initiated

511 by L2 to L3 and L18 to L22b, played a similar role. This may directly prevent L4 and  
512 L14 from successfully attaching the ground, and can also be the reason why there  
513 were no attempted leaders occurring after the last return stroke.  
514



## 5. Summary

We record an altitude-triggered lightning whose leader/return stroke sequences containing 15 attempted leaders and 8 stroked leaders, using a HS camera and a mirrorless camera. The path and velocity characteristics of them are analyzed in detail. These attempted leaders are found to die out in three ways, and a branching node is found to be the critical point between them and stroked leaders. There is no inevitable relation between the initial speed and the final fate of leaders. A watershed between these attempted leaders and stroked leaders is found to be the propagation speed value of  $4 \times 10^6 \text{ m/s}$ , which is applicable in this paper. The influence brought by a return stroke on development of the following leader processes is found to have a duality. It can promote and hinder the following leader processes at the same time. The branching behavior of these leaders is investigated, and a conclusion applicable with most of the leaders here is proposed that these leaders will slow down before producing a branch.

## Acknowledgments

This work was supported by the National Natural Science Foundation of China (Grant number: 51807144 and 51877155). The authors express their gratitude to Mr. Junfeng Wang, Prof. Yijun Zhang, Prof. Shaodong Chen, Prof. Weitao Lyu and all the members of Triggered Lightning Action 2018-2019 at Guangzhou Field Experiment Site in Conghua, Guangdong Province, China.

This study complies with the AGU data policy. The data archiving is underway and will be presented at Zenodo repository. The data has been temporarily uploaded a

538 copy of data as Supporting Information for review purposes.

539

## References

Biagi, C. J., M. A. Uman., J. D. Hill., & D. M. Jordan. (2014). Negative leader step mechanisms observed in altitude triggered lightning. *Journal of Geophysical Research: Atmospheres*, 119(13), 8160-8168, doi:10.1002/2013jd020281.

Campos, L. Z., Saraiva, A.V., Alves, J., Pinto, O., Zepka, G.S., & Buzato, T.S. (2013). On the progression of sequential attempted leaders preceding a subsequent negative stroke in a bipolar lightning flash. American Geophysical Union Fall Meeting 2013.

Huang, H., D. Wang., T. Wu., & N. Takagi. (2019). Progression Features of Dart Leaders in Natural Negative Cloud-to-Ground Lightning Flashes. *Journal of Geophysical Research: Atmospheres*, 124(21), 11143-11154, doi:10.1029/2019jd030990.

Jiang, R., Z. Wu., X. Qie., D. Wang., & M. Liu. (2014). High-speed video evidence of a dart leader with bidirectional development. *Geophysical Research Letters*, 41(14), 5246-5250, doi:10.1002/2014gl060585.

Lalande, P., A. Bondiou-Clergerie., P. Laroche., A. Eybert-Berard., J. P. Berlandis., B. Bador., et al. (1998). Leader properties determined with triggered lightning techniques. *Journal of Geophysical Research: Atmospheres*, 103(D12), 14109-14115, doi:10.1029/97jd02492.

562

563 Laroche, P., V. Idone, A. Eybert-Berard, & L. Barret. (1991). Observations of  
564 bidirectional leader development in triggered lightning flash, paper presented at the  
565 International Conference on Lightning and Static Electricity, NASA, Cocoa Beach,  
566 Fla, April 16-19, 1991

567

568 Lyu, W., Zhang, Y., Li J., Zheng, D., Dong, W., Chen, S., & Wang, F. (2008). Optical  
569 Observations on Propagation Characteristics of Leaders in Cloud-to-Ground  
570 Lightning Flashes, *Journal of Meteorological Research*, 22(1), 66-77

571

572 Lyu, W., Zhang, Y., Zhou, X., Meng, Q., Zheng, D., Ma, M., Wang, F., Chen, S., &  
573 Qie, X. (2008), Analysis of Channel Luminosity Characteristics in Rocket-Triggered  
574 Lightning, *Journal of Meteorological Research*, 22(3), 362-374

575

576 Mardiana, R., Z.-I. Kawasaki, & T. Morimoto. (2002). Three-dimensional lightning  
577 observations of cloud-to-ground flashes using broadband interferometers, *Journal of*  
578 *Atmospheric and Solar-Terrestrial Physics*, 64 (2002) 91–103

579

580 Miki, M., V. A. Rakov., T. Shido., G. Diendorfer., M. Mair., F. Heidler., et al. (2005).  
581 Initial stage in lightning initiated from tall objects and in rocket-triggered lightning.  
582 *Journal of Geophysical Research*, 110(D2), doi:10.1029/2003jd004474.

583

584 Qie, X., Y. Pu., R. Jiang., Z. Sun., M. Liu., H. Zhang., X. Li., G. Lu., & Y. Tian.  
585 (2017). Bidirectional leader development in a preexisting channel as observed in  
586 rocket-triggered lightning flashes. *Journal of Geophysical Research: Atmospheres*,  
587 122(2), 586-599, doi:10.1002/2016jd025224.

588

589 Qie, X., Zhao, Y., Zhang, Q., Yang, J., Feng, G., Kong, X., et al. (2009).  
590 Characteristics of triggered lightning during Shandong artificial triggering lightning  
591 experiment (SHATLE). *Atmospheric Research*, 91(2-4), 310-315,  
592 doi:10.1016/j.atmosres.2008.08.007.

593

594 Rakov, V. A., Uman, M. A., Rambo, K.J., Fernandez, K. J., Fisher, R. J., Schnetzer, G.  
595 H., et al. (1998). New insights into lightning processes gained from  
596 triggered-lightning experiments in Florida and Alabama. *Journal of Geophysical*  
597 *Research: Atmospheres*, 103(D12), 14117-14130, doi:10.1029/97jd02149.

598

599 Rhodes, C.T., X.M. Shao, P.R. Krehbiel, R.J. Thomas, & C.O. Hayenga. (1994)  
600 Observations of lightning phenomena using radio interferometry, *Journal of*  
601 *Geophysical Research*, 99, 13,059-13,082, 1994

602

603 Saba, M. M. F., O. Pinto, N. N. Solórzano, & A. Eybert-Berard. (2005). Lightning  
604 current observation of an altitude-triggered flash. *Atmospheric Research*, 76(1-4),  
605 402-411, doi:10.1016/j.atmosres.2004.11.005.

606

607 Shao, X. M., P. R. Krehbiel, R. J. Thomas, & W. Rison. (1995) Radio interferometric  
608 observations of cloud-to-ground lightning phenomena in Florida, *Journal of*  
609 *Geophysical Research*, 100, 2749-2783, 1995

610

611 Wang, C., Z. Sun, R. Jiang, Y. Tian, & X. Qie. (2018). Characteristics of downward  
612 leaders in a cloud-to-ground lightning strike on a lightning rod. *Atmospheric Research*,  
613 203, 246-253, doi:10.1016/j.atmosres.2017.12.014.

614

615 Wang, D., V. A. Rakov., M. A. Uman., N. Takagi., T. Watanabe., D. E. Crawford., et al.  
616 (1999). Attachment process in rocket-triggered lightning strokes. *Journal of*  
617 *Geophysical Research*, 104(D2),2143-2150

618

619 Wang, J., Q. Li, L. Cai, M. Zhou, Y. Fan, J. Xiao, & A. Sunjerga. (2019b).  
620 Multiple-station measurements of a return-stroke electric field from rocket-triggered  
621 lightning at distances of 68–126 km. *IEEE Transactions on Electromagnetic*  
622 *Compatibility*, 61(2), 440-448, doi:10.1109/temc.2018.2821193.

623

624 Yang, J., X. Qie, Q. Zhang, Y. Zhao, G. Feng, T. Zhang, & G. Zhang. (2009).  
625 Comparative analysis of the initial stage in two artificially-triggered lightning flashes.  
626 *Atmospheric Research*, 91(2-4), 393-398, doi:10.1016/j.atmosres.2008.04.010.

627

628 Zhang, G., Y. Zhao, X. Qie, T. Zhang, Y. Wang, & C. Chen. (2008). Observation and  
629 study on the whole process of cloud-to-ground lightning using narrowband radio  
630 interferometer, *Science in China Series D: Earth Sciences*, 51(5), 694-708,  
631 doi:10.1007/s11430-008-0049-9.

632

633 Zhang, Y., Dong, W., Zhang, G., & Qie, X. (2003). Characteristics of leader processes  
634 in altitude-triggered lightning. *Chinese Journal of Geophysics*, 46(4), 643-648.

635

636 Zhou, M., D. Wang, J. Wang, N. Takagi, W. R. Gamarota, M. A. Uman, D. M. Jordan,  
637 J. T. Pilkey, & T. Ngin. (2014). Correlation between the channel-bottom light intensity  
638 and channel-base current of a rocket-triggered lightning flash. *Journal of Geophysical*  
639 *Research: Atmospheres*, 119(23), 13,457-413,473, doi:10.1002/2014jd022367.

640

641 Zhu, Y., Z. Ding, V. A. Rakov, & M. D. Tran. (2019). Evolution of an Upward  
642 Negative Lightning Flash Triggered by a Distant +CG From a 257-m-Tall Tower,  
643 Including Initiation of Subsequent Strokes. *Geophysical Research Letters*, 46(12),  
644 7015-7023, doi:10.1029/2019gl0832